Bioorganic Chemistry 119 (2022) 105572

Contents lists available at ScienceDirect

Bioorganic Chemistry

journal homepage: www.elsevier.com/locate/bioorg

Novel thiophene Chalcones-Coumarin as acetylcholinesterase inhibitors: Design, synthesis, biological evaluation, molecular docking, ADMET prediction and molecular dynamics simulation

Aso Hameed Hasan [a,b], Sankaranarayanan Murugesan [c], Syazwani Itri Amran [d], Subhash Chander [e], Mohammed M. Alanazi [f], Taibi Ben Hadda [g], Sonam Shakya [h], Mohammad Rizki Fadhil Pratama [i,j], Basundhara Das [k], Subhrajit Biswas [k], Joazaizulfazli Jamalis [a,*]

[a] Department of Chemistry, Faculty of Science, Universiti Teknologi Malaysia, 81310 Johor Bahru, Johor, Malaysia
[b] Department of Chemistry, College of Science, University of Garmian, Kalar 46021, Kurdistan Region-Iraq, Iraq
[c] Medicinal Chemistry Research Laboratory, Birla Institute of Technology & Science Pilani (BITS Pilani), Pilani Campus, Pilani 333031, Rajasthan, India
[d] Department of Biosciences, Faculty of Science, Universiti Teknologi Malaysia, 81310 Johor Bahru, Johor, Malaysia
[e] Amity Inst Phytomedicine and Phytochemistry, Amity University, Amity Univ Uttar Pradesh, Noida 201313, India
[f] Department of Pharmaceutical Chemistry, College of Pharmacy, King Saud University, Riyadh 11451, Saudi Arabia
[g] Umm Al Qura University Umm Al Qura Univ, Fac Pharm, Dept Pharmaceut Chem, Mecca 21955, Almukkarramah, Saudi Arabia
[h] Department of Chemistry, Faculty of Science Aligarh Muslim University, Aligarh 202002, India
[i] Doctoral Program of Pharmaceutical Sciences, Universitas Airlangga, Jl Dr Ir Soekarno Kampus C UNAIR Mulyorejo, Surabaya, East Java 60115, Indonesia
[j] Department of Pharmacy, Universitas Muhammadiyah Palangkaraya, Jl RTA Milono Km 1.5 Pahandut, Palangka Raya, Central Kalimantan 73111, Indonesia
[k] Amity Institute of Molecular Medicine and Stem Cell Research (AIMMSCR), Translational Cancer & Stem Cell Research Laboratory, Research Laboratory 101, J3 Block, Amity University, Noida, Uttar Pradesh, India

ARTICLE INFO

Keywords:
Thiophene Chalcone
Coumarin
Acetylcholinesterase
Molecular docking
Molecular dynamics
ADMET study
Cytotoxicity

ABSTRACT

A series of around eight novel chalcone based coumarin derivatives (**23a-h**) was designed, subjected to *in-silico* ADMET prediction, synthesized, characterized by IR, NMR, Mass analytical techniques and evaluated as acetylcholinesterase (AChE) inhibitor for the treatment of Alzheimer's disease (AD). The results of predicted ADMET study demonstrated the drug-likeness properties of the titled compounds with developmental challenges in lipophilicity and solubility parameters. The *in vitro* assessment of the synthesized compounds revealed that all of them showed significant activity (IC_{50} ranging from 0.42 to 1.296 μM) towards AChE compared to the standard drug, galantamine ($IC_{50} = 1.142 \pm 0.027$ μM). Among these, compound **23e** displayed the most potent inhibitory activity with IC_{50} value of 0.42 ± 0.019 μM. Cytotoxicity of all compounds was tested on normal human hepatic (THLE-2) cell lines at three different concentrations using the MTT assay, in which none of the compound showed significant toxicity at the highest concentration of 1000 μg/ml compared to the control group. Based on the docking study against AChE, the most active derivative **23e** was orientated towards the active site and occupied both catalytic anionic site (CAS) and peripheral anionic site (PAS) of the target enzyme. *In-silico* studies revealed tested showed better inhibition activity of AChE compared to Butyrylcholinesterase (BuChE). Molecular dynamics simulation explored the stability and dynamic behavior of **23e**- AChE complex.

1. Introduction

Alzheimer's disease (AD), the most common cause of dementia in the elderly, is affecting millions of people worldwide. The ailment is characterized by a complex neurodegenerative process occurring in the central nervous system which leads to progressive cognitive decline and memory loss [1–3]. Although, the etiology of AD is not yet entirely known, some factors are reported to play key role in the pathogenesis of this disease, including low levels of neurotransmitter acetylcholine (ACh), oxidative stress, accumulation of abnormal proteins (β-amyloid

* Corresponding author.
E-mail address: joazaizulfazli@utm.my (J. Jamalis).

https://doi.org/10.1016/j.bioorg.2021.105572
Received 17 July 2021; Received in revised form 4 December 2021; Accepted 15 December 2021
Available online 21 December 2021

(βA) and τ-protein), neuroinflammation and neuronal toxicity [4–6]. For the treatment of AD, several approaches have been reported. Hence, the approved drugs up to date are; rivastigmine, donepezil, galantamine and memantine (*N*-methyl-D-aspartate (NMDA) antagonist). These drugs found to have side effects, but can only provide temperary symptomatic relief [7].

Chalcone or (*E*)-1,3-diphenyl-2-propene-1-one is considered as the important precursor of flavonoids and isoflavonoids and they are the open chain intermediate in aurone synthesis of flavones. They exist in many conjugated forms in nature possessing a benzylideneacetophenone scaffold, where the two aromatic rings are joined by three carbon having an α,β-unsaturated carbonyl linkage [8,9]. Chalcones are also used as the key intermediate in synthesizing a large number of biologically active heterocyclic compounds [10,11]. Chalcones has been reported for variety of promising biological activities such as anti-viral [12,13], anti-oxidant [14–16], anti-breast cancer [17] anti-bacterial, anti-fungal [18–23], anti-tubercular [24], analgesic [25], anti-leishmanial [26], anti-inflammatory [27,28], anti-malarial [29], anti-amoebic [30], anti-depressant, anti-convulsant [31], and monoamine oxidase inhibitory (MAOI) activity [32]. In addition, Liu reported that, reactive α,β-unsaturated keto function in chalcone moiety might play significant role for its inhibitory activity against acetylcholinesterase (AChE) [33]. Furthermore, heterocyclic compounds have been widely studied due to their interesting applications as bioactive molecules. Especially, compounds containing sulfur have attracted medicinal chemist's interest because of their therapeutics potential [34,35].

Coumarins (2*H*-chromen-2-one or 2*H*-1-benzopyran-2-one) are secondary heterocyclic metabolites, belonging to benzopyrones family which composed of fused benzene and α-pyrone rings and they occur widely in different parts of plants, such as roots, seeds, nuts, flowers and fruits [36]. Coumarin based compounds obtained from the natural and synthetic origin are well documented for the inhibition of AChE activity [37–44]. Natural products such as scopoletin, esculetin, decursinol and mesuagenin are well reported for AChE inhibition activity [45]. Inspired by the natural coumarin as inhibitors of AChE, many researchers designed and evaluated synthetic coumarin aiming to improve the inhibitory activity and selectivity towards AChE [46].

In a study reported by Amin and co-workers, twenty compounds containing 7-benzyloxycoumarin based compounds were synthesized and tested for acetylcholinesterase (AChE) inhibition, in which five compounds showed potency better than the reference drug donepezil (IC_{50}: 0.711 μM). Three compounds **1, 2** and **3** displayed significant memory improvement in scopolamine-induced impairment mice model and computational studies performed using compound **1,** illustrated binding at catalytic active site (CAS) and the peripheral anionic site (PAS) of AChE enzyme [47]. Hybrid series of nicotinonitrile-coumarin were synthesized and tested for AChE inhibition activity, in which best active compounds **4** and **5** showed 94.1 and 72.3% inhibition of AChE, respectively, at tested concentration of 25 nM, even better than the standard drug donepezil [48]. Derivatives of *N1*-(coumarin-7-yl) exhibited moderate (42.5 to 442 μM) to potent (2.0 nM to 442 μM) activity against AChE and BChE, enzymes respectively. Best active compound **6** exhibited IC_{50} of 24.25 μM and 2.0 nM against AChE and BChE, respectively [49].

Heo and team isolated fifteen khellactone-type coumarins from the roots of *Peucedanum japonicum* and *in-vitro* tested for AChE and BChE inhibition activity, in which compounds **7** and **8** inhibited activity of AChE with IC_{50} 9.28 and 7.20 μM, respectively [50].

Zhang and co-workers reported a novel series of coumarin/piperazine hybrids in which compound **9** showed potent activity against AChE as well as BChE with IC_{50} of 2.42 and 3.42 μM, respectively without any significant toxicity at the tested concentration of 100 μM [51]. Baruah and team evaluated AChE inhibitory potency of two substituted coumarin derivatives in which compound chromenyl coumarate **10** showed potent activity with IC_{50} of 48.49 nM, even superior to the reference drug donepezil IC_{50} 74.13 nM [52]. In another study, new coumaryl-thiazole derivatives were synthesized and *in vitro* evaluated for AChE inhibition activity. Best active compound of the series, compound **11** showed nanomolar potency (IC_{50} 43 nM) with selectivity of around 4151.16 times over BuChE. Compound did not showed significant cellular toxicity at the tested concentration [53]. Among the novel series of coumarin aryl amide-based compounds reported by the Yao and team, compound **12** displayed potent AChE inhibition activity with IC_{50} value of 34 nM, also showed cytoprotective against H_2O_2 induced cell death in human neuroblastoma cells [54]. Ghanei-Nasab and team investigated AChE and BuChE inhibition activity of compounds comprising of coumarin-3-carboxamide bearing tryptamine. SAR study on the scaffold revealed favorable anti-AChE activity upon insertion of benzyloxy moiety at the 7-position of coumarin scaffold, particularly, compound **13** exhibited best activity with IC_{50} value of 0.16 mM [55].

Considering the AChE inhibitory potential of coumarin based compounds, we envisioned to synthesize the series of compounds (**23a-h**) containing coumarin ring linked with thiophene chalcone system *via* aliphatic chain (Fig. 2). Initially, all the designed compounds were subjected to in-silico ADMET prediction study, followed by synthesis and characterization using spectral analytical methods. The synthesized compounds were characterized and *in-vitro* evaluated for AChE inhibition activity. Using the best active compound, docking and molecular dynamics studies were performed to estimate its putative binding mode and stability at the binding site, respectively. Relative selectivity of compounds towards AChE and Butyrylcholinesterase (BuChE) were *in-silico* tested, while toxicity of all compounds was tested on normal human hepatic cell lines (THLE-2) using the MTT assay.

2. Results and discussion

2.1. In-silico prediction of physicochemical and ADMET parameters

The physicochemical and ADMET parameters of the titled compounds were predicted *in-silico*, as shown in Table 1. The results of each were then compared with the optimum range of drug-likeness parameters presented in Table S1 that has been followed by 95% of the marketed drugs. There were two exciting parameters to observe: log P and log S. of the eight compounds, only four compounds (**23a**, **23b**, **23c** and **23e**) met the optimum prescribed value of log P. as for log S, none of the compounds included in the optimum range (highlighted by bold font). Lipophilic properties and poor solubility in water of these compounds will pose challenges in their development, especially for absorption characteristics [56]. However, with the proper formulation, these characteristics could still be handled as in clofazimine with a log P > 7 but could still be given orally [57].

The other parameters showed results in the optimum prescribed range. Apart from the distinctly different Mol Wt, other parameters whose results varied were log P, log S, Caco2, log BB, and Rot; other than that, the results of other parameters were same for all the compounds. The addition of the bromine atom at position number 2 of thiophene was not enough to significantly influence the physicochemical and AMDET properties of the compound, which has been observed while analyzing each compound in pairs (compound **23a** with **23b**, **23c** with **23d**, and so on). Even though they were not identical, the difference in the values of parameters for these pairs of compounds almost always had difference with a consistent pattern, such as in log P (difference 0.7625), Caco2 (0.011), and log BB (0.028–0.029). A significant difference was shown by log S (0.171–0.279), which was influenced by the length of methyl group, thereby affect its solubility in water [58]. For Rot, the difference was 0 because the bond with bromine was not rotating, so it did not affect the number of rotatable bonds [59].

The toxicity profile of all the compounds were relatively in safe range, with a pLD_{50} of 1500 mg/kg, and was in class IV acute toxicity based on GSH. All the compounds did not showed probability against Ames test, so they were not predicted to cause mutagenicity. Overall, based upon the *in-silico* prediction of physicochemical and ADMET

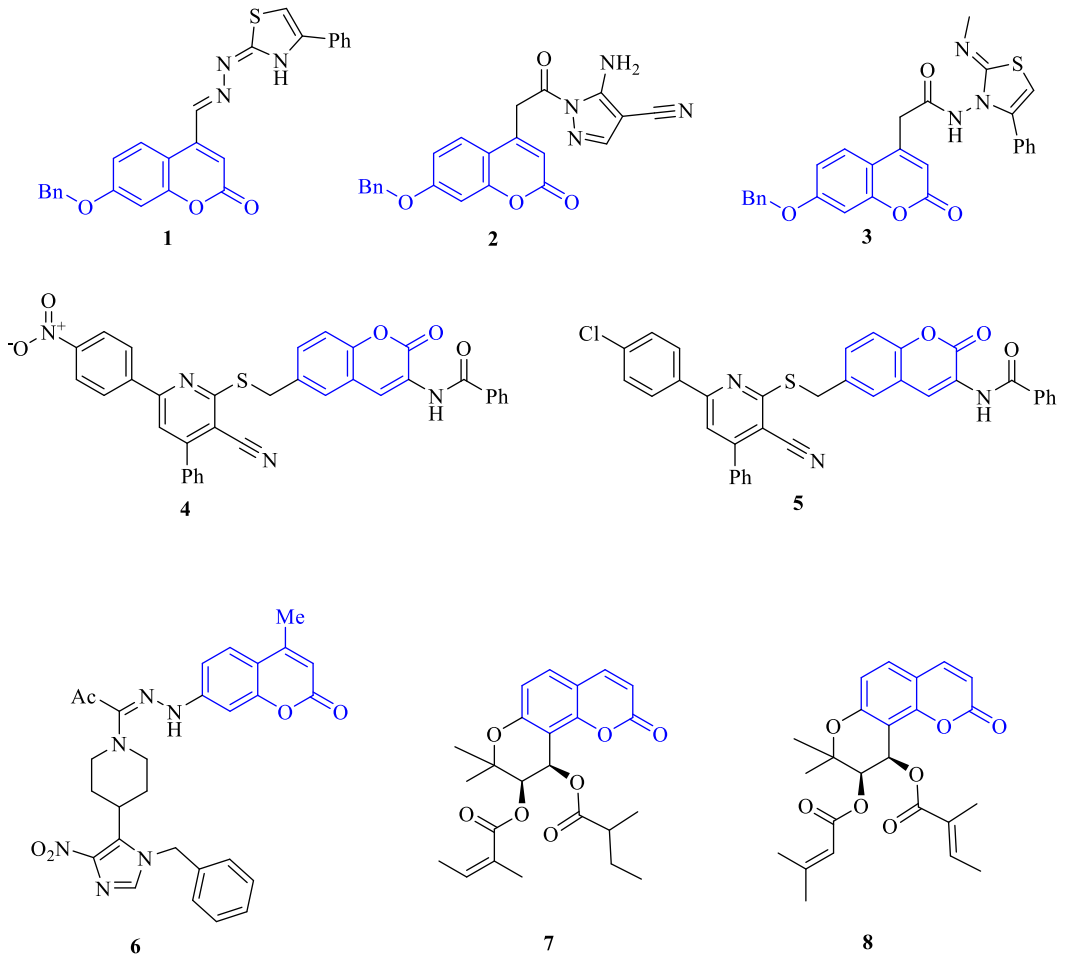

Fig. 1. Structure of compounds containing coumarin conjugated with thiazole, pyrazole, pyridine, piperidine and fused tetrahydro pyran as choline esterase inhibitory agents.

parameters of all the synthesized compounds possessed the drug-likeness properties.

2.2. Chemistry

The synthetic routes to get the designed compounds **(23a-h)** are outlined in Scheme 1.**7**-Hydroxy-4-methylcoumarin **(16)** was prepared *via* the condensation of resorcinol **(14)** with ethyl acetoacetate **(15)** in dioxane, catalyzed by sulfuric acid. The synthesis of hydroxychalcones **(20** and **21)** was carried out *via* base catalyzed Claisen-Schmidt condensation of 4-hydroxyacetophenone **(19)** with heteroaryl aldehyde **(17** and **18)** in absolute ethanol stirring overnight at room temperature. The alkylation reaction of the hydroxychalcones **(20** and **21)** with an appropriate α,ω-dibromoalkanes in the presence of catalytic amount of anhydrous K_2CO_3 and in refluxing acetonitrile successfully afforded *O*-alkylated chalcones **(22a-h)**. The designed compounds **(23a-h)** were synthesized *via* reaction of *O*-alkylated chalcones **(22a-h)** and 7-hydroxy-4-methylcomarin **(16)**, catalyzed by anhydrous potassium carbonate.

The structure of the compounds (**23a-h**) were elucidated by FT-IR, ^{1}H NMR, ^{13}C NMR and high resolution mass spectroscopy (HRMS). The FT-IR spectra of all titled compounds showed almost similar pattern. The spectra of these compounds revealed absorption bands of C—H sp^2, C—H sp^3, C═O (lactone and ketone), C═C olefinic and C═C aromatic. Two strong absorption bands of C═O (lactone) in the range 1708–1736 cm^{-1} and C═O (ketone) around 1642–1652 cm^{-1}, were reported. The ^{1}H NMR spectra of the titled compounds proved that the reaction has been successfully done by the disappearance of the triplet signal in the region δ 3.63–3.60, which was corresponded to (-CH_2Br) group in molecule structure of the intermediates **(22a-h)** and being replaced with (—CH_2O) group. The structure of target compounds (**23a-h**) were further confirmed with ^{13}C NMR analysis, among the two peaks attributable for carbonyl groups, the C═O groups for chalcone moiety was appeared in the range δ 187.69–188.08 while for coumarin it observed between δ 161.46–162.08. The spectra also displayed signals for *trans*-olefinic carbons of chalcone moiety at around δ 125.52–125.70 (C-α) and δ 135.45–136.65(C-β) [60–66]. The remaining carbon atoms were observed in the expected chemical shift region.

2.3. Biological activity evaluation

The *in vitro* anticholinesterase activity of titled compounds **23a-h** was determined against AChE. The obtained IC_{50} values (μM) were presented in Table 2. The results indicated that all titled compounds possess significant inhibitory activity in the range of 0.42–1.296 μM. Among them, (*E*)-4-methyl-7-(4-(4-(3-(thiophen-2-yl)-acryloyl)-phenoxy)-butoxy)–2*H*-chromen-2-one derivative (compound **23e)** exhibited IC_{50} of 0.42 ± 0.019 μM was most potent among the tested analogues against AChE, which is 2.5-folds most active than that of control drug galantamine (IC_{50} = 1.142 μM). From the obtained results (Table 2), it seems that the variation of the spacer length between chalcone scaffolds and coumarin significantly affected the anticholinesterase activity profile. Moreover, structure–activity relationship (SAR) study of the tested compounds revealed that the inhibitory activity is dependent on the

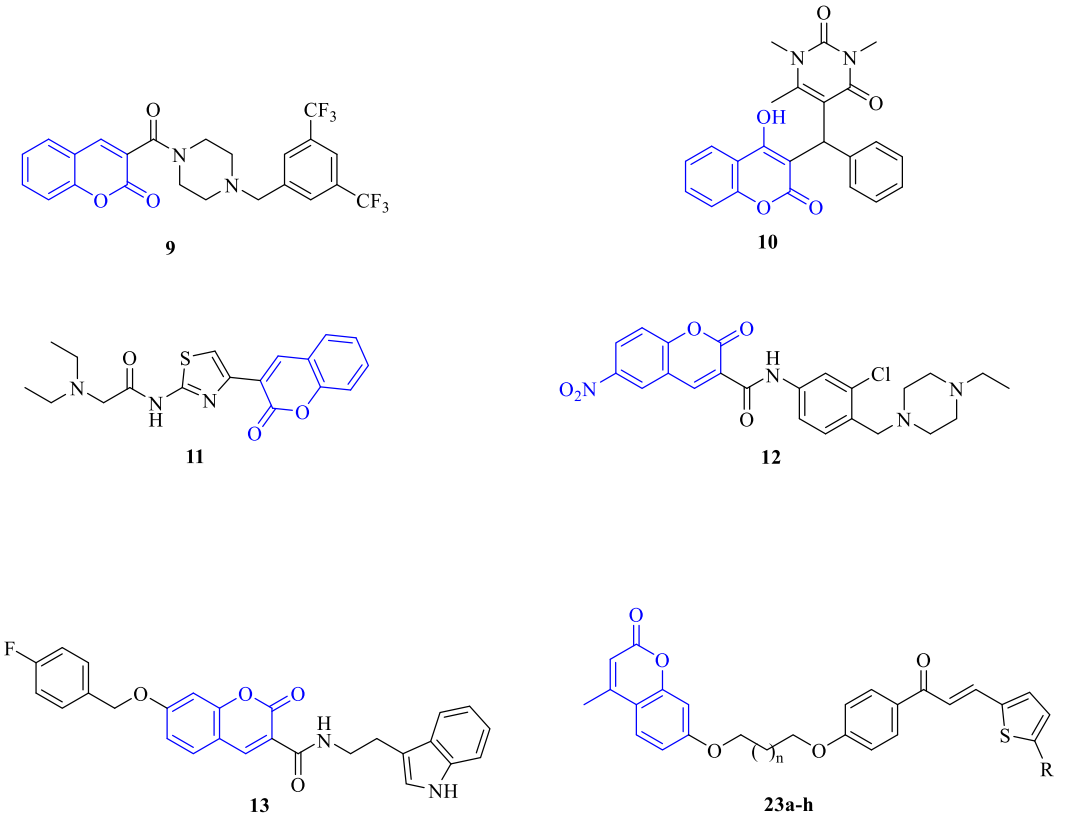

Fig. 2. Structure of compounds containing coumarin conjugated with pyrimidine-dione, thiazole, thiophene, indole and designed compounds as choline esterase inhibitory agents.

Table 1
In-silico predicted physicochemical and ADMET parameters of the titled compounds.

Compounds	Mol Wt[a]	TPSA[b]	HBD	HBA	log P	log S[c]	Caco2[d]	log BB	Rot	Acute tox.[e]	pLD_{50}[f]	Ames
23a	432.49	93.98	0	5	5.51682	**−6.946**	0.41	−0.047	8	IV	1500	No
23b	511.38	93.98	0	5	6.27932	**−7.225**	0.421	−0.076	8	IV	1500	No
23c	446.51	93.98	0	5	5.90692	**−7.183**	0.429	−0.389	9	IV	1500	No
23d	525.41	93.98	0	5	**6.66942**	**−7.427**	0.44	−0.418	9	IV	1500	No
23e	460.54	93.98	0	5	6.29702	**−7.334**	0.379	−0.485	10	IV	1500	No
23f	539.44	93.98	0	5	**7.05952**	**−7.541**	0.39	−0.513	10	IV	1500	No
23g	474.57	93.98	0	5	**6.68712**	**−7.384**	0.329	−0.546	11	IV	1500	No
23h	553.46	93.98	0	5	**7.44962**	**−7.555**	0.34	−0.574	11	IV	1500	No

[a] Molecular weight in g/mol.
[b] Topological polar surface area in $Å^2$.
[c] Aqueous solubility in log mol/L.
[d] Predicted apparent Caco-2 cell permeability in 10^{-6} cm/s.
[e] Acute toxicity according to the globally harmonized system (GHS) of classification and labeling of Chemicals.
[f] Predicted LD_{50} in mg/kg.

substituents present on the thiophene ring and the length of linker. The compound **23a** with two methylene spacer revealed significant inhibitory activity against the target enzyme. The insertion of bromo group on thiophene ring as in compound **23b** resulted in reduced anticholinesterase activity. In contrast, the activity could be retained by increasing one carbon unit to the compound **23a**, gave compound **23c**. Generally, compounds (**23a**, **23c**, **23e** and **23g**) with no substituent exhibited parabola profile potencies against AChE with the growth of carbon units. Whereas compounds (**23b**, **23d**, **23f** and **23h**) with bromo group on thiophene ring showed dramatically declined in potencies while increasing the carbon chain linker. Meanwhile, *in silico* study proved that all the designed compounds effectively inhibit ChEs in the nanomolar to micromolar range. As presented in Table 2 compounds showed better inhibition constant against AChE over the BuChE enzyme.

2.4. Docking studies

Compounds **23a-h** exhibited binding free energy (ΔGb) in the range of −10.00 to −11.40 kcal/mol compared to −9.60 kcal/mol for the control compound (galantamine). In order to better understand the putative binding mode at the active site of the target protein, molecular docking study for the most active compound **(23e)** was performed against the active site of the target enzyme AChE (PDB code: 4EY7). As shown in Fig. 3, the coumarin moiety occupied the catalytic anionic site (CAS) of the enzyme, connected *via* two hydrogen bonds between carbonyl oxygen with residues GLY121 and GLY122. Meanwhile, at the peripheral anionic site (PAS) region another two hydrogen bonds were also observed between carbonyl oxygen of chalcone moiety and amino acid residues TYR72 and TRP286. The phenyl ring of coumarin

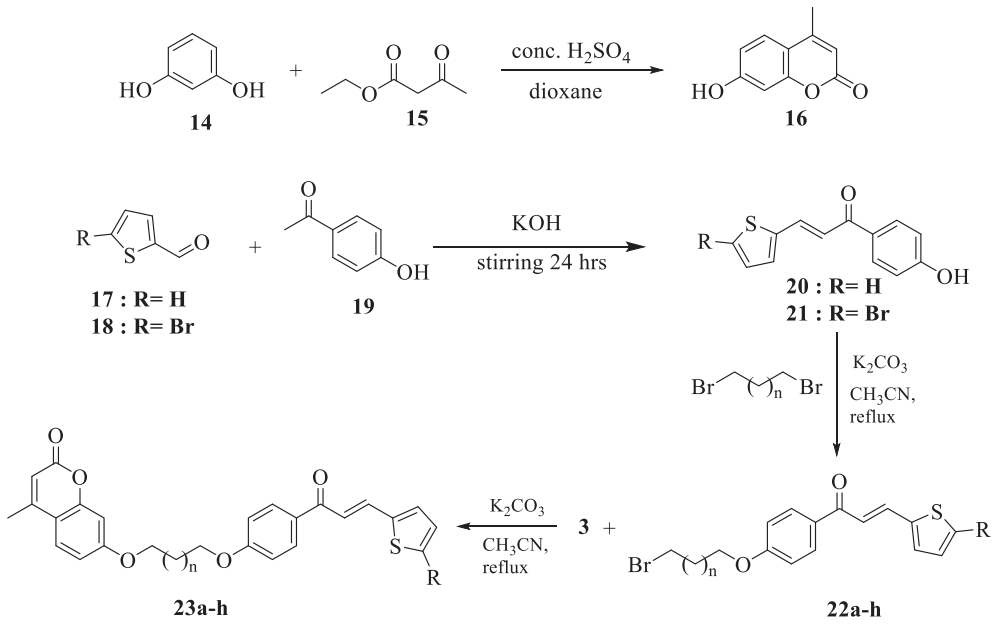

Scheme 1. Synthesis of the titled compounds **(23a-h)**.

Table 2
Inhibition of AChE by the titled compounds **23a-h**.

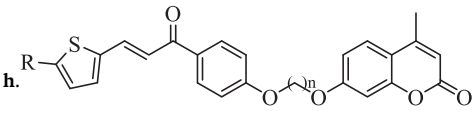

23a-h

Comp.	R	n	*In Vitro*	*In silico*		SI*
			IC_{50} [μM] AChE	IC_{50} [μM] AChE	IC_{50} [μM] BuChE	
23a	H	2	0.699 ± 0.054	2.11	44.82	0.0471
23b	Br	2	0.786 ± 0.052	0.36222	43.46	0.0083
23c	H	3	0.486 ± 0.039	1.81	73.65	0.0246
23d	Br	3	0.823 ± 0.094	1.35	77.92	0.0173
23e	H	4	0.420 ± 0.019	1.31	65.5	0.0200
23f	Br	4	1.237 ± 0.012	0.36523	20.46	0.0179
23 g	H	5	0.512 ± 0.007	1.32	48.45	0.0272
23 h	Br	5	1.296 ± 0.026	0.27208	55.73	0.0049
Galantamine			1.142 ± 0.027			

* SI: Selectivity Index.

established two π-π *T*-shaped interactions with TYR337 and TYR341 amino acid residues. Another two π-π *T*-shaped interactions were also found between HIS447 and methyl substituent, between thiophene ring of chalcone core and HIS287 amino acid residue. While another phenyl ring of chalcone was able to form two π-π stacking interactions with residue TRP286. The methyl group of coumarin core produced interactions with TYR337 and TRP86 *via* π-alkyl interactions. Amino acid HIS447 showed π-alkyl and electrostatic (π-cation) interactions with pyrone ring of coumarin. A *π*-sulfur interaction was found between the sulfur atom and HIS287 amino acid residue.

2.5. *In vitro cytotoxicity evaluation of synthesized compounds*

Cytotoxicity of all synthesized compounds was evaluated against normal human hepatic (THLE-2) cell lines using the MTT assay at three different concentrations 0.25, 0.5 and 1 mg/ml. [67]. Negative control used in the study comprises of alone medium without any test compound.

As demonstrated in Fig. 4, no significant difference in cell viability was observed in the treated wells with respect to control group even at the highest concentration, i.e, 1000 μg/ml of compounds. Hence, these compounds cause minimal to no cytotoxicity to the transformed normal human liver cell line.

2.6. *Molecular dynamics (MD) simulation*

The best-posed model with the highest docking score obtained from Auto Vina for the protein–ligand complex was used as starting structure for 100 ns MD simulation (Fig. 5). Only the best docking output has been used to set up this process in high-throughput manner and to analyze the binding mechanism dynamics of the ligand at the active site of protein under clearly expressed water conditions. The conformational change analysis of the protein–ligand complex was analyzed during the 1, 10, 20, 50 and 100 ns MD production run as shown in Fig. 6. The minimum change in ligand conformation was noticed at 1 ns, maximum at 50 ns, and very slight at 100 ns. Molecular dynamics data are processed by calculating the root mean square deviation (RMSD) (from the starting structure) to analyze the structural stability. The RMSD value of the compound was found to be ~2.58 Å (Fig. 7). From the RMSD plot, it can be seen that the complex formed stable conformation from ~50 ns with suitable RMSD value of ~2.5 Å. The most acceptable RMSD value range was <3.0 Å, as the lower RMSD value indicates superior stability of the system [68]. The root mean square fluctuation (RMSF) of the protein–ligand complex was plotted from 100 ns MD trajectory to analyze the average fluctuation and flexibility of individual amino acid (Fig. 8). The RMSF plot indicates that amino acid residue fluctuations are present in the protein during ligand-bound state at several time intervals. The results depict that the interaction of ligand and protein brings protein chains closer and leads to reduction in the distance between them which is represented in Fig. 9**(a).** The residue-residue (RR) distance map (two-dimensional representations of protein 3D structure) is shown in Fig. 9 **(b)** that plot the patterns of spatial interactions between amino acid

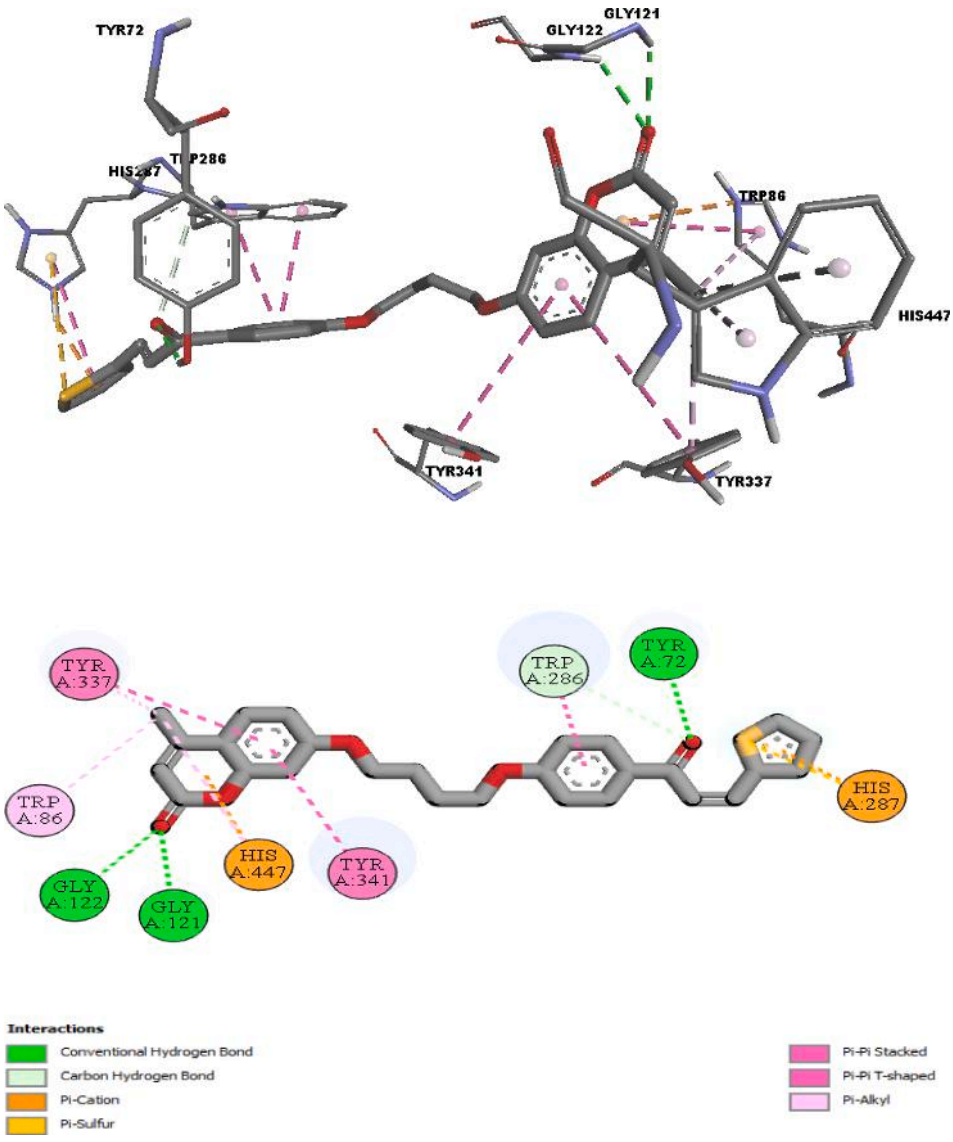

Fig. 3. 3D and 2D binding site interactions of compound **23e** at the active site of target protein (PDB ID: 4EY7).

residues [69,70]. The compactness of the ligand bound protein was analyzed by radius of gyration (Rg) plot. From the obtained results, a decrease in Rg for protein–ligand complex along the simulation time was observed, showing an increase in the compactness of the structure (Fig. 10).

The number of hydrogen bond interactions occurred between protein and ligand were calculated with grid-search on 16x16x19 grid, rcut = 0.35 and plotted against time as shown in Fig. 11. Upon calculation of hydrogen bonds between protein (5270 atoms) and ligand (43 atoms), 737 donors and 1472 acceptors were found. The average number of hydrogen bonds per timeframe was observed to be 1.493 out of 542,432 possible. During overall analysis, it was found that ligand–-protein interaction significantly increased the number of hydrogen bonds. The solvent accessible surface area (SASA) of the protein was calculated during MD simulation in ligand-bound conditions. SASA values changed due to binding of ligand to the protein (Fig. 12). The analysis indicates the folding states of protein and its stability upon ligand binding.

3. Experimental

3.1. In-silico prediction of physicochemical and ADMET parameters

Prediction of physicochemical and ADMET properties of the titled compounds was carried out *in silico* with a combination of several web servers such as SwissADME, pkCSM, and ProTox-II, with the procedure as reported by our previous study [71]. Several critical parameters were predicted as reported by Chander [72,73], including molecular weight (Mol Wt.), topological polar surface area (TPSA), number of hydrogen bond donor (HBD), number of hydrogen bond acceptor (HBA), octanol/water partition coefficient (log P), aqueous solubility (log S), Caco-2 permeability (Caco2), brain/blood partition coefficient (log BB), number of rotatable bonds (Rot), acute toxicity (Acute tox.), predicted LD_{50} (pLD_{50}), and Ames mutagenicity (AMES).

3.2. Chemistry

3.2.1. Materials and methods

All the chemicals were purchased from Sigma-Aldrich and Merk. All chemicals and reagents were of analytical grade and were used without further purification. Melting points (uncorrected) were determined

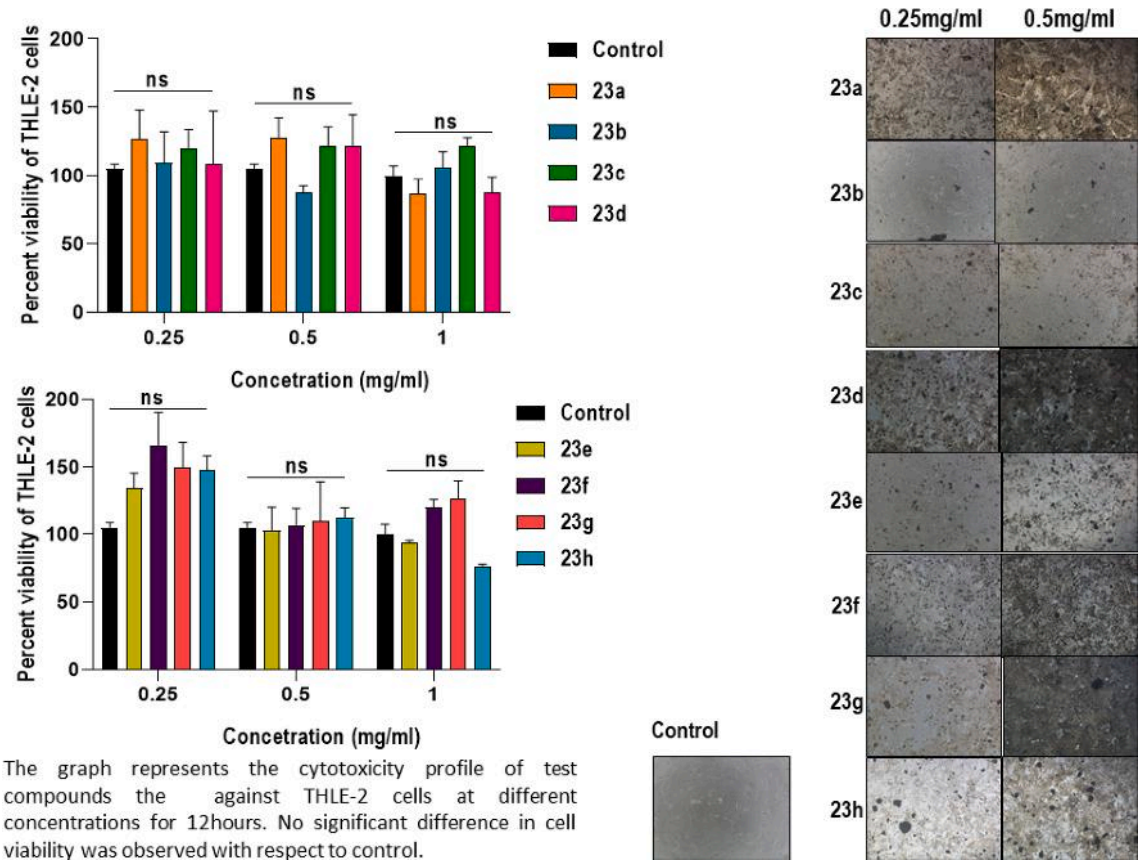

Fig. 4. Cytotoxicity profile of the compounds against THLE-2 cells at different concentrations for 12 h.

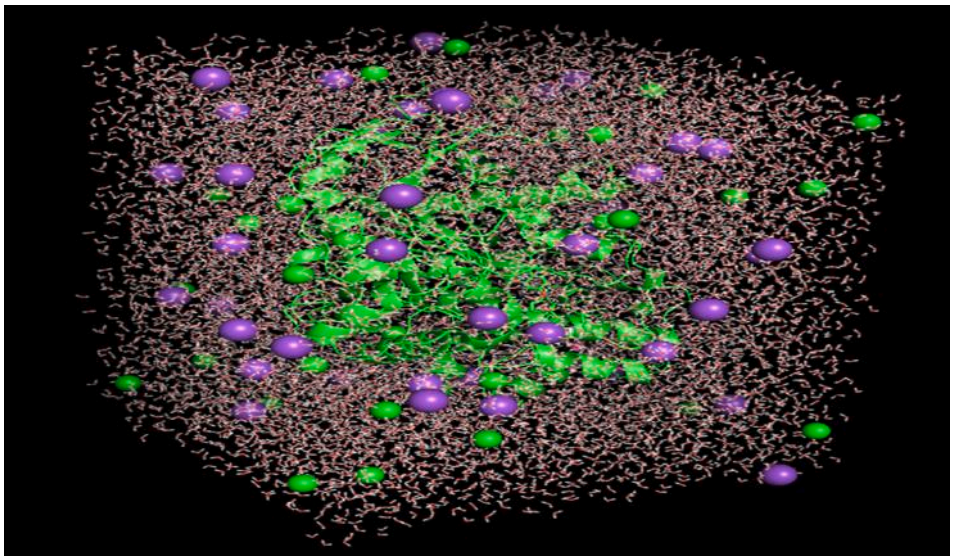

Fig. 5. Protein-ligand complex in triclinic box solvated with water molecules and neutralized with Na^+ and Cl^- ions (0.15 M salt).

using a Barnstead Electrothermal 9100 melting point. Infrared (IR) spectra were recorded on Perkin Elmer FT-IR spectrometer. Samples were prepared as KBr disc. The ^1H NMR (400 MHz) and ^{13}C NMR (175 MHz) were recorded on Bruker Avance II Spectrometer using TMS as an internal standard. Chemical shift values were given in δ (ppm) scales. The HRMS were recorded on Agilent Technologies 6545 Q-TOF LC/MS. Thin layer chromatography (TLC) was performed using alumina sheets pre-coated with silica gel 60 F254 (0.2 mm thickness) in order to monitor as well as detect compounds and the spots were visualized under UV lamp at 254 nm.

*3.2.2. Synthesis of 7-Hydroxy-4-methylcoumarin (**16**)*

Concentrated H_2SO_4 (1 mL) was slowly to an ice-cold solution of resorcinol (4.0 g, 36.37 mmol) in dioxane (20 mL) under 25 ℃. Ethyl acetoacetate (6.0 g, 48.96 mmol) was added to the reaction mixture and refluxed for 4 h. After cooling to room temperature, the mixture was poured into crushed ice and stirred for another 30 min. The resulting yellow precipitate was collected by vacuum filtration, washed several

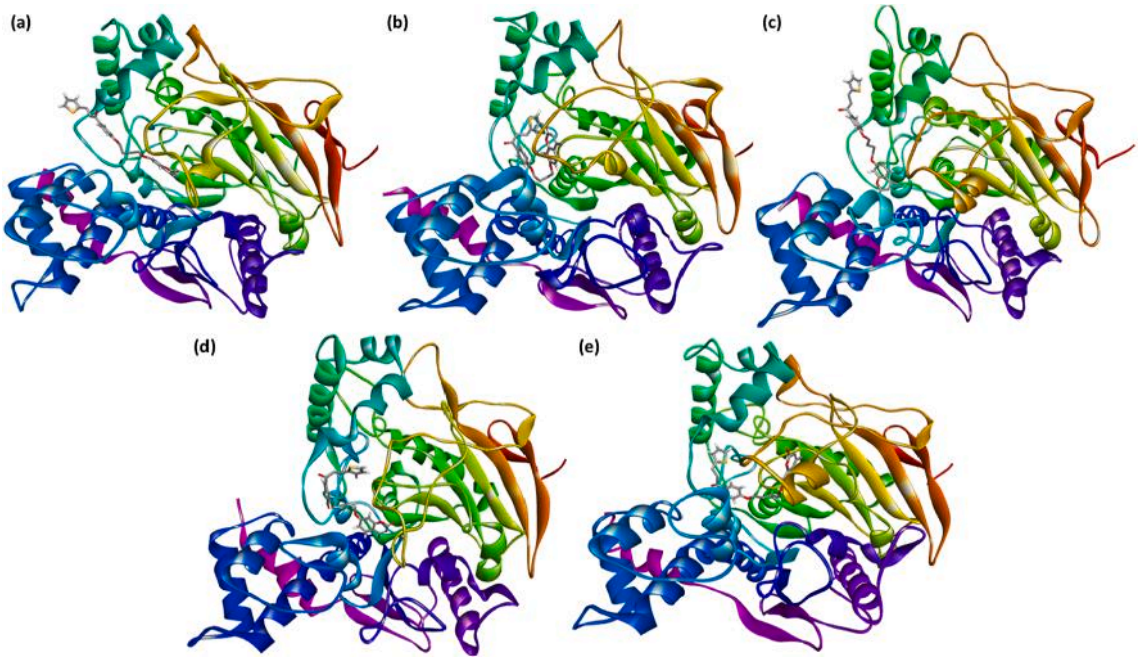

Fig. 6. Protein-ligand structure at **(a)** 1 ns, **(b)** 10 ns, **(c)** 20 ns, **(d)** 50 ns and **(e)** 100 ns MD run.

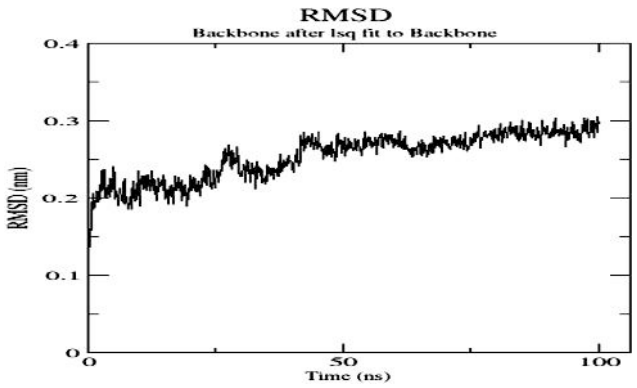

Fig. 7. The root mean square deviation (RMSD) of solvated protein backbone and ligand complex during 100 ns MD simulation.

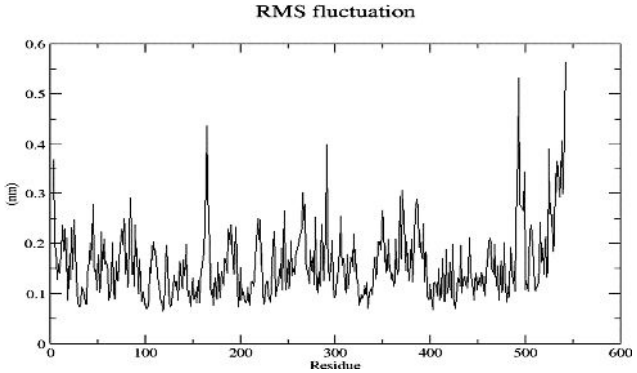

Fig. 8. The root mean square fluctuation (RMSF) values of solvated protein–ligand complex plotted against residue numbers.

times with water and dried in an oven. The product was subjected to re-crystallization from methanol yielded 7-hydroxy-4-methyl-2*H*-chromen-2-one **(16)**.

*3.2.3. General procedure for the synthesis of 4′-Hydroxychalcones (**20** and **21**)*

A mixture of 4′-hydroxyacetophenone **(19)** (10 mmol) and 2-thiophenecarboxaldehyde/5-bromothiophene-2-carbaldehyde (12 mmol) was dissolved in solution of absolute ethanol (25 mL) and 25% KOH (5 mL). The reaction mixture was stirred for 24 h at room temperature. The solution was poured into cold water and acidified with concentrated HCl. The precipitate was collected, washed several times with water and dried. The product was subjected to re-crystallization from ethanol (96%) to afford 4′-hydroxychalcones **(20** and **21)**.

*3.2.4. General procedure of synthesis of intermediates (**22a-h**)*

A mixture of chalcones **(20 or 21**) (2 mmol), an appropriate α,ω-dibromoalkanes (10 mmol), and anhydrous K_2CO_3 (450 mg) was dissolved in acetonitrile (50 mL). The reaction mixture was refluxed for 7 h and was then poured into cold water (50 mL). Immediately the precipitate was formed, filtrate off, washed with cold water, and dried in an oven gave compounds **(22a-h).**

*3.2.5. General procedure for the synthesis of hybrids (**23a-h**)*

A mixture of *O*-alkylated chalcones **(22a-h)** (1 mmol) and 7-hydroxy-4-methylcomarin (**16**) (1 mmol) was dissolved in acetonitrile (30 mL) and anhydrous K_2CO_3 (200 mg) was added. The reaction mixture was refluxed overnight. After that, the reaction mixture was cooled down to room temperature and poured into 25 mL of cold water. Immediately, the precipitates were formed, filtrate off, washed with cold water, and dried in an oven to give chalcone-coumarin analogues **(23a-h)**.

3.3. Biological evaluation of hybrids against acetylcholine esterase (AChE)

The assay for AChE inhibitory activity of the titled compounds was done based on slightly modified protocol reported by Yang et al. [74]. AChE (E.C.3.1.1.7, Type VI-S, from Electric Eel), 5,5′-dithiobis-2-nitrobenzoic acid (Ellman's reagent, DTNB) and acetylthiocholine chloride (ATCI) were purchased form Sigma Aldrich. Enzyme solutions were prepared to give 0.28 units/mL aliquots. Stock solutions were prepared by dissolving 1 mg of test compounds in 1 mL of DMSO and diluted to

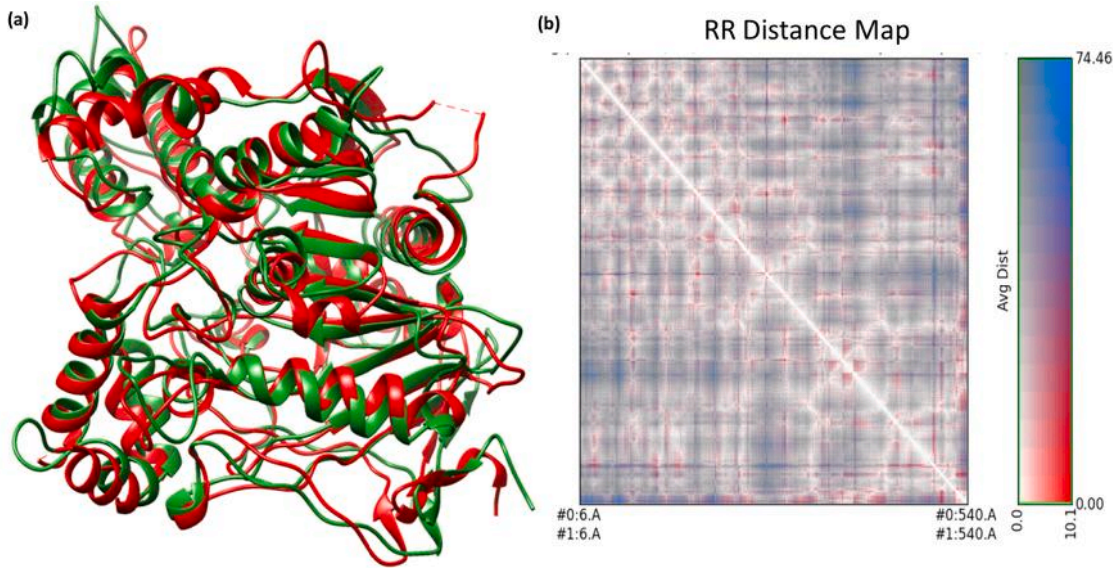

Fig. 9. (a) Superimposed structure of unbounded protein (red) and protein–ligand complex (green);**(b).** Residue-Residue (RR) distance map pattern display the spatial interactions of protein.

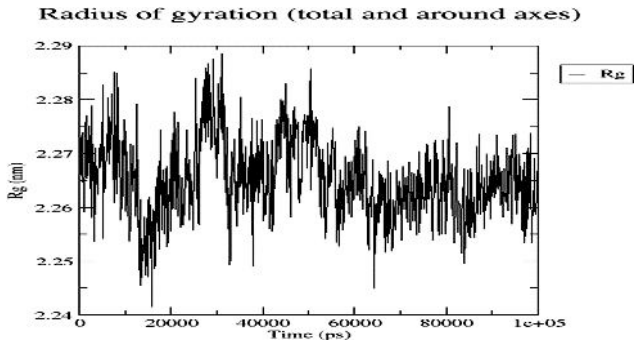

Fig. 10. Radius of gyration (Rg) of protein–ligand complex during 100 ns simulation time.

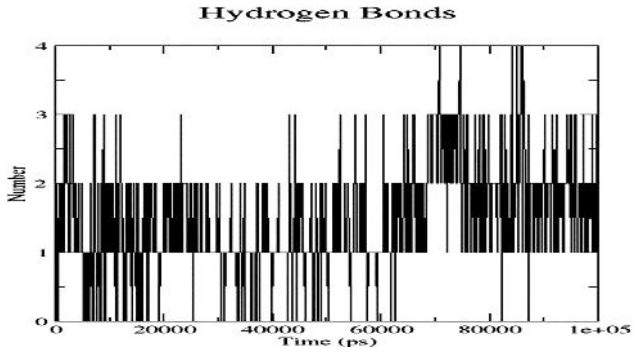

Fig. 11. Number of average hydrogen bonding interaction between protein–ligand complex during 100 ns simulation time.

final concentration of 1000, 800, 600, 400, 200, 100 and 50 μg/mL. The assay buffer solution (pH = 8.0) was prepared from taking 93.20 mL of solution (6 g of sodium dihydrogen phosphate was dissolved in 500 mL of deionized water) mixed with 6.80 mL of solution (7 g of sodium hydrogen phosphate was dissolved in 500 mL of deionized water) and adjusted. Otherwise, 57.70 mL of sodium dihydrogen phosphate and 42.30 mL of sodium hydrogen phosphate was mixed and adjusted to prepare buffer (pH = 7.0). Furthermore, fresh solution of 0.01 M DTNB

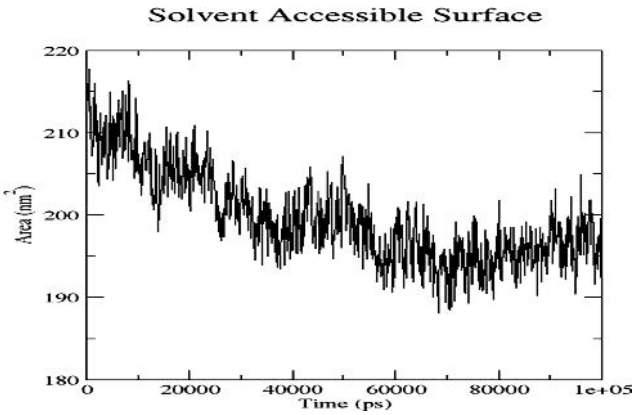

Fig. 12. Solvent accessible surface area (SASA) analysis for protein–ligand complex during 100 ns simulation time.

(0.396 g of DTNB and 15 mg $NaHCO_3$ were dissolved in 100 mL of buffer pH 7.0) in dark place, and 0.075 M ATCI (0.2048 g of ATCI was dissolved in 10 mL of deionized water), were prepared. In 96-well plates, 20 μL of the test compounds, 10 μL of DTNB, 15 μL of enzyme (AChE) and 140 μL of buffer solution (pH = 8.0), were added in dark condition and incubated for 15 min. after that, followed by the addition of ATCI (10 μL) and incubated again for the same period. The activity was measured by reading absorbance of solution at 412 nm. Blanks containing all components except enzyme were carried out. IC_{50} values were calculated as concentration of compound that produces 50% enzyme activity inhibition, using the GraphPad Prism 8 program package. Results are expressed as the mean ± SD of at least three different experiments performed in triplicate.

3.4. Molecular docking study

All calculations were performed using AutoDock Vina [75]. The 3D crystallographic structures of target enzymes AChE (PDB ID: 4EY7 [76] and BuChE (PDB ID: 4BDS [77] were downloaded from the RSCB Protein Data Bank (https://www.rcsb.org). The preparation of enzymes was carried out by removing the co-crystallized ligand and water molecules, the polar hydrogen atoms were added. The Avogadro program [78] was

used for drawing the 3D structure of target compounds and energy minimizations. Discovery Studio 2.5 software (Accelrys Inc., San Diego, CA, USA) was used for docking analysis and to generate the 2D/3D binding modes of compounds.

3.5. In vitro cytotoxicity assay

Normal human liver cells, THLE-2 (purchased from ATCC) were usually cultured at Dr. Biswas lab at AIMMSCR, Amity University in DMEM-F12 (HiMedia) media supplemented with 10% FBS (HiMedia), 70 ng/ml of phosphoethanolamine (TCI Chemicals), 5 ng/ml of epidermal growth factor (Gibco), Insulin Transferrin Selenium (ThermoScientific, diluted to 1X), Penicillin-Streptomycin solution, 100 μg/ml (HiMedia), at 5 %CO_2 in a CO_2 incubator. Experiments were carried out when cells were 70–80% confluent. To perform the cell viability assay, 96-well plate (SPL) was coated with collagen peptide and incubated for 2–3 h prior to cell seeding. $5x10^3$ of THLE-2 cells were resuspended in complete medium as described above and seeded in each well. After 24 h, the media was carefully aspirated from the wells. Stock solution of all designed compounds were prepared in DMSO. Cells were treated with respective drugs dissolved in complete culture medium at different concentrations for 12 h. MTT (3-(4,5-Dimethylthiazol-2-yl)-2,5-diphenyltetrazolium bromide) reagent (HiMedia) with a final concentration of 0.5 mg/mL was added to each well and further incubated for 4 h. Equal volume of DMSO (SRL) was added in each well to solubilize the formazan crystals with a final incubation of 15–20 min. Absorbance was measured using Multiskan Microplate Reader (ThermoScientific) at 570 nm wavelength. All experiments were performed in triplicates.

3.6. Molecular dynamics (MD) simulation

Protein-ligand complex identified from molecular docking study was subjected to molecular dynamics (MD) simulation and to evaluate their inhibitory potential and conformational space. The GROMACS (GROningen MAchine for Chemical Simulations) version 2019.2 package was used to perform molecular dynamics simulation analysis with GROMOS96 43a1 force field. Ligand topology and parameter files were generated using the latest CGenFF via CHARMM-GUI [79,80]. Protein-ligand structures were solvated in a triclinic box using simple point-charge (SPC) water models that extended 10 Å from the protein [81]. Na^+ and Cl^- ions (0.15 M salt) were used to neutralize the systems (Fig. 1). The system was subjected to periodic boundary conditions in the Canonical ensemble (NVT): moles (N), volume (V) and temperature (T)/Isothermal-Isobaric (NPT) ensemble: moles (N), pressure (P) and temperature (T) (NPT/NVT) equilibration run at constant temperature (300 K) and pressure (1.0 bar) using Leap-frog MD integrator for 100 ns simulation time [82]. The particle-mesh Ewald method was used for electrostatic interactions [83]. The force-based switching function was used to truncate non-bonded interactions over 10 and 12 Å [84]. Bad contact inside the system was discarded by energy minimization through the steepest descent method with 5000 steps. In addition, temperature coupling was applied by indexing the system into water and non-water components to avoid hot solvent-cold solute problem. Also, modified Berendsen thermostat and Parrinello-Rahman barostat were employed for NVT and NPT equilibrations. GROMACS analysis tools were used to perform trajectory analysis. The root mean square fluctuations (RMSF) and root mean square deviation (RMSD) of protein were calculated using gmxrmsf and gmx rms tools, respectively. The radius of gyration (Rg) and solvent accessible surface area (SASA) was computed by gmx gyrate and gmxsasa tools, respectively. Further, gmxhbond tool was employed to analyze hydrogen bonds. Plots were prepared using Grace Software and PyMol & VMD were used for the visualization of the complex structure [85,86]. Our simulations were conducted using processor Intel(R) Xeon(R) CPU E5-2680 v4 @ 2.40 GHz, 64 bit. The simulation time for the protein–ligand complex was 36.9 h for 100 ns. The MD simulation's speed is orders of magnitude slower than computational docking.

4. Conclusion

In conclusion, we designed, *in-silico* predicted ADMET parameetrs and synthesized a new series of chalcone-coumarin hybrids as acetylcholinesterase inhibitor. The titled compounds were synthesized, characterized by IR, NMR and Mass spectral analysis. The *in vitro* assessment displayed that all the titled compounds (expect of compounds **23f** and **23h**) exhibited superior inhibitory activity towards AChE than that of standard drug galantamine. Obtained results exhibited that the linker length connecting chalcone moiety and coumarin core played an important role in AChE inhibition. Moreover, insertion of bromo group on C-5 of thiophene ring in chalcone moiety led to decrease in AChE inhibition activity. *In* the *vitro* studies, none of the compound showed significant toxicity in normal human hepatic cell up to the highest tested concentration of 1000 μg/ml. *In silico* studies revealed more selective inhibitory potential of compounds towards AChE compared to BuAChE. The molecular docking studies of most active compound **23e** revealed that this compound can fit into the PAS and CAS regions of the target enzyme's dual active sites. AChE inhibitory activity of this compound could further be optimized to find a suitable drug candidate for the management of AD. The 100 ns MD simulation study revealed that the protein–ligand complex possesses stable conformation and lower protein–ligand interaction energy. Hence, the identified compound may be considered as lead for further study in the search of novel AChE inhibitory agent. The right formulation will be needed to improve the drug-like properties of these compounds, especially their lipophilicity and solubility.

Declaration of Competing Interest

The authors declare that they have no known competing financial interests or personal relationships that could have appeared to influence the work reported in this paper.

Acknowledgments

The authors wish to thank Universiti Teknologi Malaysia and the Ministry of Higher Education (MOHE) Malaysia for funding this research under the Fundamental Research Grant Scheme (FRGS/1/2019/STG01/UTM/02/7).

Appendix A. Supplementary material

Supplementary data to this article can be found online at https://doi.org/10.1016/j.bioorg.2021.105572.

References

[1] 2010 Alzheimer's disease facts and figures, Alzheimer's & Dementia 6(2) (2010) 158–194. https://doi.org/10.1016/j.jalz.2010.01.009.
[2] B. Benhamú, M. Martín-Fontecha, H. Vázquez-Villa, L. Pardo, M.L. López-Rodríguez, Serotonin 5-HT6 Receptor Antagonists for the Treatment of Cognitive Deficiency in Alzheimer's Disease, J. Med. Chem. 57 (17) (2014) 7160–7181, https://doi.org/10.1021/jm5003952.
[3] L. Piazzi, A. Rampa, A. Bisi, S. Gobbi, F. Belluti, A. Cavalli, M. Recanatini, 3-(4-{[benzyl(methyl)amino]methyl}-phenyl)-6,7-dimethoxy-2H-2-chromenone (AP2238) inhibits both acetylcholinesterase and acetylcholinesterase-induced β-amyloid aggregation: A dual function lead for Alzheimer's disease therapy, J. Med. Chem. 46 (12) (2003) 2279–2282, https://doi.org/10.1021/jm0340602.
[4] B. Brus, U. Košak, S. Turk, A. Pišlar, N. Coquelle, J. Kos, J. Stojan, J.-P. Colletier, S. Gobec, Discovery, Biological Evaluation, and Crystal Structure of a Novel Nanomolar Selective Butyrylcholinesterase Inhibitor, J. Med. Chem. 57 (19) (2014) 8167–8179, https://doi.org/10.1021/jm501195e.
[5] S. Sinha, I. Lieberburg, Cellular mechanisms of β-amyloid production and secretion, PNAS 96 (20) (1999) 11049–11053, https://doi.org/10.1073/pnas.96.20.11049.

[6] L. Wang, R. Zeng, X. Pang, Q. Gu, W. Tan, The mechanisms of flavonoids inhibiting conformational transition of amyloid-β42 monomer: a comparative molecular dynamics simulation study, RSC Adv. 5 (81) (2015) 66391–66402, https://doi.org/10.1039/c5ra12328c.

[7] P. Thapa, S.P. Upadhyay, W.Z. Suo, V. Singh, P. Gurung, E.S. Lee, R. Sharma, M. Sharma, Chalcone and its analogs: Therapeutic and diagnostic applications in Alzheimer's disease, Bioorg. Chem. 108 (2021) 104681, https://doi.org/10.1016/j.bioorg.2021.104681.

[8] H.M. Al-Maqtari, J. Jamalis, H.M. Sirat, Synthesis and characterization of heterocyclic chalcones containing halogenated thiophenes, Jurnal Teknologi 77 (3) (2015) 55–59, https://doi.org/10.11113/jt.v77.6005.

[9] H.P. Ávila, E.d.F.A. Smânia, F.D. Monache, A. Smânia, Structure–activity relationship of antibacterial chalcones, Bioorg. Med. Chem. 16 (22) (2008) 9790–9794, https://doi.org/10.1016/j.bmc.2008.09.064.

[10] B.E. Aksöz, R. Ertan, Spectral properties of chalcones II, Fabad J. Pharm. Sci 37 (4) (2012) 205–216.

[11] R. Kalirajan, S. Sivakumar, S. Jubie, B. Gowramma, B. Suresh, Synthesis and biological evaluation of some heterocyclic derivatives of chalcones, Int. J. Chem. Tech. Res. 1 (1) (2009) 27–34.

[12] J.C. Trivedi, J.B. Bariwal, K.D. Upadhyay, Y.T. Naliapara, S.K. Joshi, C. C. Pannecouque, E. De Clercq, A.K. Shah, Improved and rapid synthesis of new coumarinyl chalcone derivatives and their antiviral activity, Tetrahedron Lett. 48 (48) (2007) 8472–8474, https://doi.org/10.1016/j.tetlet.2007.09.175.

[13] J.-H. Wu, X.-H. Wang, Y.-H. Yi, K.-H. Lee, Anti-AIDS agents 54. A potent anti-HIV chalcone and flavonoids from genus Desmos, Bioorg. Med. Chem. Lett. 13 (10) (2003) 1813–1815, https://doi.org/10.1016/S0960-894X(03)00197-5.

[14] R.J. Anto, K. Sukumaran, G. Kuttan, M.N.A. Rao, V. Subbaraju, R. Kuttan, Anticancer and antioxidant activity of synthetic chalcones and related compounds, Cancer Lett. 97 (1) (1995) 33–37, https://doi.org/10.1016/0304-3835(95)03945-S.

[15] S. Mukherjee, V. Kumar, A.K. Prasad, H.G. Raj, M.E. Bracke, C.E. Olsen, S.C. Jain, V.S. Parmar, Synthetic and biological activity evaluation studies on novel 1,3-diarylpropenones, Bioorg. Med. Chem. 9 (2) (2001) 337–345, https://doi.org/10.1016/S0968-0896(00)00249-2.

[16] G. Vanangamudi, M. Subramanian, G. Thirunarayanan, Synthesis, spectral linearity, antimicrobial, antioxidant and insect antifeedant activities of some 2,5-dimethyl-3-thienyl chalcones, Arabian J. Chem. 10 (2017) S1254–S1266, https://doi.org/10.1016/j.arabjc.2013.03.006.

[17] V.R. Solomon, H. Lee, Anti-breast cancer activity of heteroaryl chalcone derivatives, Biomed. Pharmacother. 66 (3) (2012) 213–220, https://doi.org/10.1016/j.biopha.2011.11.013.

[18] H.M. Al-Maqtari, J. Jamalis, T.B. Hadda, M. Sankaranarayanan, S. Chander, N. A. Ahmad, H. Mohd Sirat, I.I. Althagafi, Y.N. Mabkhot, Synthesis, characterization, POM analysis and antifungal activity of novel heterocyclic chalcone derivatives containing acylated pyrazole, Res. Chem. Intermed. 43 (3) (2017) 1893–1907, https://doi.org/10.1007/s11164-016-2737-y.

[19] O. Mazimba, Antimicrobial activities of heterocycles derived from thienylchalcones, J. King Saud Univ. – Sci. 27 (1) (2015) 42–48, https://doi.org/10.1016/j.jksus.2014.06.003.

[20] L.S. Ming, J. Jamalis, H.M. Al-Maqtari, M.M. Rosli, M. Sankaranarayanan, S. Chander, H.-K. Fun, Synthesis, characterization, antifungal activities and crystal structure of thiophene-based heterocyclic chalcones, Chem. Data Collect. 9–10 (2017) 104–113, https://doi.org/10.1016/j.cdc.2017.04.004.

[21] Z. Nowakowska, A review of anti-infective and anti-inflammatory chalcones, Eur. J. Med. Chem. 42 (2) (2007) 125–137, https://doi.org/10.1016/j.ejmech.2006.09.019.

[22] Y.R. Prasad, P.P. Kumar, P.R. Kumar, A.S. Rao, Synthesis and antimicrobial activity of some new chalcones of 2-acetyl pyridine, E-J. Chem. 5 (1) (2008) 144–148, https://doi.org/10.1155/2008/602458.

[23] A. Usta, A. Yaşar, N. Yılmaz, C. Güleç, N. Yaylı, Ş. Karaoğlu, N. Yaylı, Synthesis, Configuration, and Antimicrobial Properties of Novel Substituted and Cyclized '2′,3″-Thiazachalcones', Helv. Chim. Acta 90 (8) (2007) 1482–1490, https://doi.org/10.1002/hlca.200790154.

[24] P.M. Sivakumar, S.K.G. Babu, D. Mukesh, QSAR studies on chalcones and flavonoids as anti-tuberculosis agents using genetic function approximation (GFA) method, Chem. Pharm. Bull. 55 (1) (2007) 44–49, https://doi.org/10.1248/cpb.55.44.

[25] G. Viana, M. Bandeira, F. Matos, Analgesic and antiinflammatory effects of chalcones isolated from Myracrodruon urundeuva Allemão, Phytomedicine 10 (2–3) (2003) 189–195, https://doi.org/10.1078/094471103321659924.

[26] F.F. Barsoum, H.M. Hosni, A.S. Girgis, Novel bis(1-acyl-2-pyrazolines) of potential anti-inflammatory and molluscicidal properties, Bioorg. Med. Chem. 14 (11) (2006) 3929–3937, https://doi.org/10.1016/j.bmc.2006.01.042.

[27] J.F. Ballesteros, M.J. Sanz, A. Ubeda, M.A. Miranda, S. Iborra, M. Paya, M. J. Alcaraz, Synthesis and Pharmacological Evaluation of 2'-Hydroxychalcones and Flavones as Inhibitors of Inflammatory Mediators Generation, J. Med. Chem. 38 (14) (1995) 2794–2797, https://doi.org/10.1021/jm00014a032.

[28] S.-J. Won, C.-T. Liu, L.-T. Tsao, J.-R. Weng, H.-H. Ko, J.-P. Wang, C.-N. Lin, Synthetic chalcones as potential anti-inflammatory and cancer chemopreventive agents, Eur. J. Med. Chem. 40 (1) (2005) 103–112, https://doi.org/10.1016/j.ejmech.2004.09.006.

[29] X. Wu, P. Wilairat, M.-L. Go, Antimalarial activity of ferrocenyl chalcones, Bioorg. Med. Chem. Lett. 12 (17) (2002) 2299–2302, https://doi.org/10.1016/S0960-894X(02)00430-4.

[30] A. Budakoti, M. Abid, A. Azam, Synthesis and antiamoebic activity of new 1-N-substituted thiocarbamoyl-3,5-diphenyl-2-pyrazoline derivatives and their Pd(II) complexes, Eur. J. Med. Chem. 41 (1) (2006) 63–70, https://doi.org/10.1016/j.ejmech.2005.06.013.

[31] Z. Ozdemir, H.B. Kandilci, B. Gumusel, U. Calis, A.A. Bilgin, Synthesis and Studies on Antidepressant and Anticonvulsant Activities of Some 3-(2-Thienyl)pyrazoline Derivatives, Arch. Pharm. 341 (11) (2008) 701–707, https://doi.org/10.1002/ardp.200800068.

[32] S. Zaib, S. Umar Farooq Rizvi, S. Aslam, M. Ahmad, M. Al-Rashida, J. Iqbal, Monoamine oxidase inhibition and molecular modeling studies of piperidyl-thienyl and 2-pyrazoline derivatives of chalcones, Med. Chem. 11 (5) (2015) 497–505, https://doi.org/10.2174/1573406410666141229101130.

[33] H. Liu, L. Liu, X. Gao, Y. Liu, W. Xu, W. He, H. Jiang, J. Tang, H. Fan, X. Xia, Novel ferulic amide derivatives with tertiary amine side chain as acetylcholinesterase and butyrylcholinesterase inhibitors: the influence of carbon spacer length, alkylamine and aromatic group, Eur. J. Med. Chem. 126 (2017) 810–822, https://doi.org/10.1016/j.ejmech.2016.12.003.

[34] P.N. Kalaria, S.C. Karad, D.K. Raval, A review on diverse heterocyclic compounds as the privileged scaffolds in antimalarial drug discovery, Eur. J. Med. Chem. 158 (2018) 917–936, https://doi.org/10.1016/j.ejmech.2018.08.040.

[35] S.S. Saleh, S.S. Al-Salihi, I.A. Mohammed, Biological activity Study for some heterocyclic compounds and their impact on the gram positive and negative bacteria, Energy Procedia 157 (2019) 296–306, https://doi.org/10.1016/j.egypro.2018.11.194.

[36] K.N. Venugopala, V. Rashmi, B. Odhav, Review on natural coumarin lead compounds for their pharmacological activity, Biomed Res. Int. 2013 (2013) 1–14, https://doi.org/10.1155/2013/963248.

[37] P. Anand, B. Singh, N. Singh, A review on coumarins as acetylcholinesterase inhibitors for Alzheimer's disease, Bioorg. Med. Chem. 20 (3) (2012) 1175–1180, https://doi.org/10.1016/j.bmc.2011.12.042.

[38] S. Hamulakova, M. Kozurkova, K. Kuca, Coumarin Derivatives in Pharmacotherapy of Alzheimeŕ s Disease, Curr. Org. Chem. 21 (7) (2017) 602–612, https://doi.org/10.2174/1385272820666160601155411.

[39] A.H. Hasan, S.I. Amran, F.H. Saeed Hussain, B.A. Jaff, J. Jamalis, Molecular Docking and Recent Advances in the Design and Development of Cholinesterase Inhibitor Scaffolds: Coumarin Hybrids, ChemistrySelect 4 (48) (2019) 14140–14156, https://doi.org/10.1002/slct.201903607.

[40] B.Z. Kurt, I. Gazioglu, F. Sonmez, M. Kucukislamoglu, Synthesis, antioxidant and anticholinesterase activities of novel coumarylthiazole derivatives, Bioorg. Chem. 59 (2015) 80–90, https://doi.org/10.1016/j.bioorg.2015.02.002.

[41] M.R. Loizzo, R. Tundis, F. Menichini, F. Menichini, Natural products and their derivatives as cholinesterase inhibitors in the treatment of neurodegenerative disorders: an update, Curr. Med. Chem. 15 (12) (2008) 1209–1228, https://doi.org/10.2174/092986708784310422.

[42] Z. Najafi, M. Mahdavi, M. Saeedi, E. Karimpour-Razkenari, N. Edraki, M. Sharifzadeh, M. Khanavi, T. Akbarzadeh, Novel tacrine-coumarin hybrids linked to 1, 2, 3-triazole as anti-Alzheimer's compounds: In vitro and in vivo biological evaluation and docking study, Bioorg. Chem. 83 (2019) 303–316, https://doi.org/10.1016/j.bioorg.2018.10.056.

[43] A. Rastegari, H. Nadri, M. Mahdavi, A. Moradi, S.S. Mirfazli, N. Edraki, F. H. Moghadam, B. Larijani, T. Akbarzadeh, M. Saeedi, Design, synthesis and anti-Alzheimer's activity of novel 1, 2, 3-triazole-chromenone carboxamide derivatives, Bioorg. Chem. 83 (2019) 391–401, https://doi.org/10.1016/j.bioorg.2018.10.065.

[44] F. Vafadarnejad, M. Mahdavi, E. Karimpour-Razkenari, N. Edraki, B. Sameem, M. Khanavi, M. Saeedi, T. Akbarzadeh, Design and synthesis of novel coumarin-pyridinium hybrids: In vitro cholinesterase inhibitory activity, Bioorg. Chem. 77 (2018) 311–319, https://doi.org/10.1016/j.bioorg.2018.01.013.

[45] E. Jameel, T. Umar, J. Kumar, N. Hoda, Coumarin: A Privileged Scaffold for the Design and Development of Antineurodegenerative Agents, Chem. Biol. Drug Des. 87 (1) (2016) 21–38, https://doi.org/10.1111/cbdd.12629.

[46] S. Hamulakova, L. Janovec, M. Hrabinova, K. Spilovska, J. Korabecny, P. Kristian, K. Kuca, J. Imrich, Synthesis and biological evaluation of novel tacrine derivatives and tacrine–coumarin hybrids as cholinesterase inhibitors, J. Med. Chem. 57 (16) (2014) 7073–7084, https://doi.org/10.1021/jm5008648.

[47] K.M. Amin, D.E. Abdel Rahman, H. Abdelrasheed Allam, H.H. El-Zoheiry, Design and synthesis of novel coumarin derivatives as potential acetylcholinesterase inhibitors for Alzheimer's disease, Bioorg. Chem. 110 (2021) 104792, https://doi.org/10.1016/j.bioorg.2021.104792.

[48] A.E.M. Mekky, S.M.H. Sanad, Synthesis and in vitro study of new coumarin derivatives linked to nicotinonitrile moieties as potential acetylcholinesterase inhibitors, J. Heterocycl. Chem. 57 (12) (2020) 4278–4290, https://doi.org/10.1002/jhet.4134.

[49] M.N. Abu-Aisheh, A. Al-Aboudi, M.S. Mustafa, M.M. El-Abadelah, S.Y. Ali, Z. Ul-Haq, M.S. Mubarak, Coumarin derivatives as acetyl- and butyrylcholinestrase inhibitors: An in vitro, molecular docking, and molecular dynamics simulations study, Heliyon 5 (4) (2019) e01552, https://doi.org/10.1016/j.heliyon.2019.e01552.

[50] J.H. Heo, B.H. Eom, H.W. Ryu, M.-G. Kang, J.E. Park, D.-Y. Kim, J.-H. Kim, D. Park, S.-R. Oh, H. Kim, Acetylcholinesterase and butyrylcholinesterase inhibitory activities of khellactone coumarin derivatives isolated from Peucedanum japonicum Thurnberg, Sci. Rep. 10 (1) (2020), https://doi.org/10.1038/s41598-020-78782-5.

[51] J. Zhang, C.-S. Jiang, Synthesis and evaluation of coumarin/piperazine hybrids as acetylcholinesterase inhibitors, Med. Chem. Res. 27 (6) (2018) 1717–1727, https://doi.org/10.1007/s00044-018-2185-x.

[52] P. Baruah, G. Basumatary, S.O. Yesylevskyy, K. Aguan, G. Bez, S. Mitra, Novel coumarin derivatives as potent acetylcholinesterase inhibitors: insight into

efficacy, mode and site of inhibition, J Biomol Struct Dyn 37 (7) (2019) 1750–1765, https://doi.org/10.1080/07391102.2018.1465853.
[53] F. Sonmez, B. Zengin Kurt, I. Gazioglu, L. Basile, A. Dag, V. Cappello, T. Ginex, M. Kucukislamoglu, S. Guccione, Design, synthesis and docking study of novel coumarin ligands as potential selective acetylcholinesterase inhibitors, J. Enzyme Inhib. Med. Chem. 32 (1) (2017) 285–297, https://doi.org/10.1080/14756366.2016.1250753.
[54] D. Yao, J. Wang, G. Wang, Y. Jiang, L. Shang, Y. Zhao, J. Huang, S. Yang, J. Wang, Y. Yu, Design, synthesis and biological evaluation of coumarin derivatives as novel acetylcholinesterase inhibitors that attenuate H2O2-induced apoptosis in SH-SY5Y cells, Bioorg. Chem. 68 (2016) 112–123, https://doi.org/10.1016/j.bioorg.2016.07.013.
[55] S. Ghanei-Nasab, M. Khoobi, F. Hadizadeh, A. Marjani, A. Moradi, H. Nadri, S. Emami, A. Foroumadi, A. Shafiee, Synthesis and anticholinesterase activity of coumarin-3-carboxamides bearing tryptamine moiety, Eur. J. Med. Chem. 121 (2016) 40–46, https://doi.org/10.1016/j.ejmech.2016.05.014.
[56] K.T. Savjani, A.K. Gajjar, J.K. Savjani, Drug Solubility: Importance and Enhancement Techniques, ISRN Pharmaceut. 2012 (2012) 1–10, https://doi.org/10.5402/2012/195727.
[57] E. Valinetz, H. Stankiewicz Karita, P.S. Pottinger, R. Jain, Novel Administration of Clofazimine for the Treatment of Mycobacterium avium Infection, Open Forum Infect. Dis. 7 (6) (2020), https://doi.org/10.1093/ofid/ofaa183.
[58] F. Ditzinger, D.J. Price, A.R. Ilie, N.J. Köhl, S. Jankovic, G. Tsakiridou, S. Aleandri, L. Kalantzi, R. Holm, A. Nair, C. Saal, Lipophilicity and hydrophobicity considerations in bio-enabling oral formulations approaches – a PEARRL review, J. Pharmacy Pharmacol. 71 (4) (2018) 464–482, https://doi.org/10.1111/jphp.12984.
[59] D.F. Veber, S.R. Johnson, H.-Y. Cheng, B.R. Smith, K.W. Ward, K.D. Kopple, Molecular Properties That Influence the Oral Bioavailability of Drug Candidates, J. Med. Chem. 45 (12) (2002) 2615–2623, https://doi.org/10.1021/jm020017n.
[60] A.-H. Adel, E.-S. Ahmed, M.A. Hawata, E.R. Kasem, M.T. Shabaan, Synthesis and antimicrobial evaluation of some chalcones and their derived pyrazoles, pyrazolines, isoxazolines, and 5, 6-dihydropyrimidine-2-(1H)-thiones, Monatshefte für Chemie-Chemical Monthly 138 (9) (2007) 889–897, https://doi.org/10.1007/s00706-007-0700-8.
[61] B.S. Kitawat, M. Singh, R.K. Kale, Solvent free synthesis, characterization, anticancer, antibacterial, antifungal, antioxidant and SAR studies of novel (E)-3-aryl-1-(3-alkyl-2-pyrazinyl)-2-propenone, New J. Chem. 37 (8) (2013) 2541–2550, https://doi.org/10.1039/C3NJ00308F.
[62] S. Kulathooran, B. Selvakumar, M. Dhamodaran, Synthesis and biological activities of novel heterocyclic chalcone derivatives by two different methods using anhydrous potassium carbonate as an efficient catalyst, Der Pharma Chemica 6 (3) (2014) 240–249.
[63] M. Rani, Y. Mohamad, Synthesis, studies and in vitro antibacterial activity of some 5-(thiophene-2-yl)-phenyl pyrazoline derivatives, J. Saudi Chem. Soc. 18 (5) (2014) 411–417, https://doi.org/10.1016/j.jscs.2011.09.002.
[64] M. Rani, M. Yusuf, S.A. Khan, P. Sahota, G. Pandove, Synthesis, studies and in-vitro antibacterial activity of N-substituted 5-(furan-2-yl)-phenyl pyrazolines, Arabian J. Chem. 8 (2) (2015) 174–180, https://doi.org/10.1016/j.arabjc.2010.10.036.
[65] T.-D. Tran, T.-T.-N. Nguyen, T.-H. Do, T.-N.-P. Huynh, C.-D. Tran, K.-M. Thai, Synthesis and Antibacterial Activity of Some Heterocyclic Chalcone Analogues Alone and in Combination with Antibiotics, Molecules 17 (6) (2012) 6684–6696, https://doi.org/10.3390/molecules17066684.
[66] A. Usta, A. Yaşar, N. Yılmaz, C. Güleç, N. Yaylı, Ş. Karaoğlu, N. Yaylı, Synthesis, Configuration, and Antimicrobial Properties of Novel Substituted and Cyclized '2′, 3 ″-Thiazachalcones', Helv. Chim. Acta 90 (8) (2007) 1482–1490, https://doi.org/10.1002/hlca.200790154.
[67] X. Li, H. Wang, Z. Lu, X. Zheng, W. Ni, J. Zhu, Y. Fu, F. Lian, N. Zhang, J. Li, H. Zhang, F. Mao, Development of Multifunctional Pyrimidinylthiourea Derivatives as Potential Anti-Alzheimer Agents, J. Med. Chem. 59 (18) (2016) 8326–8344, https://doi.org/10.1021/acs.jmedchem.6b00636.
[68] I. Kufareva, R. Abagyan, Methods of protein structure comparison, Methods Mol. Biol. 857 (2012) 231–257, https://doi.org/10.1007/978-1-61779-588-6_10.
[69] M.D. Khan, S. Shakya, H.H. Thi Vu, L. Habte, J.W. Ahn, Low concentrated phosphorus sorption in aqueous medium on aragonite synthesized by carbonation of seashells: Optimization, kinetics, and mechanism study, J. Environ. Manage. 280 (2021) 111652, https://doi.org/10.1016/j.jenvman.2020.111652.
[70] S. Wu, Y. Zhang, A comprehensive assessment of sequence-based and template-based methods for protein contact prediction, Bioinformatics 24 (7) (2008) 924–931, https://doi.org/10.1093/bioinformatics/btn069.
[71] M.R.F. Pratama, H. Poerwono, S. Siswodiharjo, ADMET properties of novel 5-O-benzoylpinostrobin derivatives, J. Basic Clin. Physiol. Pharmacol. 30 (6) (2019), https://doi.org/10.1515/jbcpp-2019-0251.
[72] S. Chander, P. Ashok, Y.-T. Zheng, P. Wang, K.S. Raja, A. Taneja, S. Murugesan, Design, synthesis and in-vitro evaluation of novel tetrahydroquinoline carbamates as HIV-1 RT inhibitor and their antifungal activity, Bioorg. Chem. 64 (2016) 66–73, https://doi.org/10.1016/j.bioorg.2015.12.005.
[73] S. Chander, P. Wang, P. Ashok, L.-M. Yang, Y.-T. Zheng, S. Murugesan, Rational design, synthesis, anti-HIV-1 RT and antimicrobial activity of novel 3-(6-methoxy-3,4-dihydroquinolin-1(2H)-yl)-1-(piperazin-1-yl)propan-1-one derivatives, Bioorg. Chem. 67 (2016) 75–83, https://doi.org/10.1016/j.bioorg.2016.05.009.
[74] Z. Yang, D. Zhang, J. Ren, M. Yang, S. Li, Acetylcholinesterase inhibitory activity of the total alkaloid from traditional Chinese herbal medicine for treating Alzheimer's disease, Med. Chem. Res. 21 (6) (2012) 734–738, https://doi.org/10.1007/s00044-011-9582-8.
[75] O. Trott, A.J. Olson, AutoDock Vina: improving the speed and accuracy of docking with a new scoring function, efficient optimization, and multithreading, J. Comput. Chem. 31 (2) (2010) 455–461, https://doi.org/10.1002/jcc.21334.
[76] J. Cheung, M.J. Rudolph, F. Burshteyn, M.S. Cassidy, E.N. Gary, J. Love, M. C. Franklin, J.J. Height, Structures of Human Acetylcholinesterase in Complex with Pharmacologically Important Ligands, J. Med. Chem. 55 (22) (2012) 10282–10286, https://doi.org/10.1021/jm300871x.
[77] F. Nachon, E. Carletti, C. Ronco, M. Trovaslet, Y. Nicolet, L. Jean, P.-Y. Renard, Crystal structures of human cholinesterases in complex with huprine W and tacrine: elements of specificity for anti-Alzheimer's drugs targeting acetyl- and butyryl-cholinesterase, Biochem. J 453 (3) (2013) 393–399, https://doi.org/10.1042/BJ20130013.
[78] M.D. Hanwell, D.E. Curtis, D.C. Lonie, T. Vandermeersch, E. Zurek, G.R. Hutchison, Avogadro: an advanced semantic chemical editor, visualization, and analysis platform, J. Cheminf. 4 (1) (2012) 17, https://doi.org/10.1186/1758-2946-4-17.
[79] K. Vanommeslaeghe, E. Hatcher, C. Acharya, S. Kundu, S. Zhong, J. Shim, E. Darian, O. Guvench, P. Lopes, I. Vorobyov, A.D. Mackerell, CHARMM general force field: A force field for drug-like molecules compatible with the CHARMM all-atom additive biological force fields, J. Comput. Chem. (2010) NA–NA, https://doi.org/10.1002/jcc.21367.
[80] W. Yu, X. He, K. Vanommeslaeghe, A.D. MacKerell, Extension of the CHARMM general force field to sulfonyl-containing compounds and its utility in biomolecular simulations, J. Comput. Chem. 33 (31) (2012) 2451–2468, https://doi.org/10.1002/jcc.23067.
[81] W.L. Jorgensen, J. Chandrasekhar, J.D. Madura, R.W. Impey, M.L. Klein, Comparison of simple potential functions for simulating liquid water, J. Chem. Phys. 79 (2) (1983) 926–935, https://doi.org/10.1063/1.445869.
[82] M.P. Allen, D.J. Tildesley, Computer Simulation of Liquids, Oxford University Press, 2017.
[83] U. Essmann, L. Perera, M.L. Berkowitz, T. Darden, H. Lee, L.G. Pedersen, A smooth particle mesh Ewald method, J. Chem. Phys. 103 (19) (1995) 8577–8593, https://doi.org/10.1063/1.470117.
[84] P.J. Steinbach, B.R. Brooks, New spherical-cutoff methods for long-range forces in macromolecular simulation, J. Comput. Chem. 15 (7) (1994) 667–683, https://doi.org/10.1002/jcc.540150702.
[85] W.L. DeLano, S. Bromberg, PyMOL user's guide, DeLano Scientific LLC, 2004, p. 629.
[86] W. Humphrey, A. Dalke, K. Schulten, VMD: Visual molecular dynamics, J. Mol. Graph. 14 (1) (1996) 33–38, https://doi.org/10.1016/0263-7855(96)00018-5.